JOURNAL OF MATERIALS SCIENCE 4 (1969) 613–624

Massively Defective Crystalline Solutions in Fluorite-structure Oxides: the Systems ThO_2-Ln_2O_3 (Ln = La^{3+}, Gd^{3+}, Yb^{3+})

A. M. DINESS
Office of Naval Research, Washington, DC, USA

RUSTUM ROY
Material Research Laboratory, The Pennsylvania State University, University Park, Pennsylvania, USA

Received 24 January 1969

Subsolidus phase relations have been defined in three representative rare earth sesquioxide (La_2O_3, Gd_2O_3, Yb_2O_3)–thoria systems over a wide range of compositions by X-ray methods (from phase detection and precision lattice parameter measurements). Characterisation of the point defects in these fluorite structure materials shows good agreement between calculated anion vacancy models and density values measured. Currently accepted crystal chemical generalisations were found to be inadequate to rationalise phase equilibria and crystalline solubility limits in these systems.

1. Introduction

Delineation of equilibria, crystalline solubility limits and anion vacancy characters for materials in the subsolidus region of ThO_2-rare earth oxide (La_2O_3, Gd_2O_3, Yb_2O_3) systems are described in this paper. Previous work on rare earth oxide (Ln_2O_3)-thoria systems (cited below) is limited with respect to the stability relations of high purity well-equilibrated samples. Structural data, phase equilibria and point defect descriptions are essentially representations of the crystal chemical and thermodynamic characteristics of a system. In solid-solid reaction kinetics studies these thermodynamic restrictions are structure-dominated, and limit the number of reasonable reaction paths considerably. Thus, prior to such kinetic investigations, this study was necessary to elucidate the restrictions of long-range periodicity relationships between products and reactants, and to describe the defect character of fluorite phases in order to character hypothesise possible routes of ionic rearrangements.

Information in the literature suggested that ThO_2 fluorite-structure crystalline solutions were excellent examples of anion-vacant materials [1]. Indeed, the technological importance of these materials depends upon their high temperature stability and point defect content. They have been used in determinations of molar free energies of formation of compounds and of ionic transport numbers in oxides [2]. Indications of defect type in these crystalline solutions have been assigned on the basis of diffusion studies [3] and their use as solid electrolytes in high-temperature fuel cells [4]. Further, the C-type Ln_2O_3 structure approaches that of the fluorite structure and its eight-fold co-ordination of cations [5]. In the C-type structure cations are in six-fold co-ordination with their nearest neighbour anions; each anion is surrounded tetrahedrally by four cations. However, the anions are arranged at the corners of a cube, with two corners of the cube remaining empty. On the basis of this strong structural relationship and defect information it was hypothesised that massively defective crystalline solutions would form in Ln_2O_3-ThO_2 systems. The term "massively defective" is used to describe those phases in which the basic fluorite arrangement persists in

spite of deviation from stoichiometry in the range of several at. %. Thus, within a given volume, the number of anions and/or cations depart markedly from the nominal 2:1 ratio in fluorite. There is no doubt – as indeed our data will show – that at particular temperatures in particular systems the defects will order to particular derivative structures, so that the stoichiometry over which a given substructure is stable (at a given t and p) may be limited. This in no way detracts from the importance of the general considerations of the familial defect patterns, represented as disordered overall defects in fluorite, which is likely to be the real case at high temperature.

The characterisation of fluorite-structure oxide phases, including temperature and composition dependence of structural relations and defect content, was a goal of this research, as was the testing of several existing correlations of crystalline solubility with crystal chemical parameters.

2. Experimental

2.1. Preparation of Original Mixtures

Known impurity levels of starting materials (with respect to cations) were of the order of one part per thousand or less, as confirmed by emission spectroscopy and/or X-ray fluorescence methods. The technique found to be most effective for preparing mixtures of well-defined composition was co-precipitation of nitrate solutions, containing desired ratios of cations as amorphous gels with ammonium hydroxide [6]. These gels were aged, filtered and washed before being slowly dehydrated at 80 to 95° C to prevent spattering. The resulting material was mixed and ground by adding plastic balls to the powder in a plastic vial inserted in a Spex Mixer Mill.

2.2. Temperature and Pressure Environments

Starting mixtures were dried at 800° C for 5 to 10 min in noble metal containers. Long heating times (of the order of weeks at 1500° C and 12 to 48 h near 1800° C) were employed in an attempt to reach equilibrium. All subsequent studies were conducted on these samples pre-reacted at approximately 1850° C.

Initially, several compositions in each system under study were heated for ½ h at 1850° C on Pt–Rh alloys in a strip furnace [7, 8]. Estimated quench rates of 1000° C/sec were achieved by turning off the power. A preliminary interpretation of X-ray diffraction tracings taken for each of the quenched materials lent encouragement to continuing this line of investigation. A series of isothermal runs at 1800° C (using modifications of the standard quenching furnace) was conducted on the pre-reacted mixtures by firing each composition either in a Pt–40% Rh alloy bucket or in 2.5 mm diameter noble metal alloy tubes, crimped or arc welded shut. Temperature variation along such samples was estimated to be a maximum of − 3° C at a distance of 1 cm above or below the centre of the hot zone. Checking of the attainment of equilibrium assemblages was performed by approaching desired isotherms from above and below with specimens pre-fired at temperatures lower and higher than final run temperatures. Samples rapidly quenched after heat treatment were dried at 110° C and then examined.

In several instances, in order to elucidate the shape of phase diagram boundaries, small samples were heated on the strip furnace to temperatures as high as 2400° C for 15 min. Ir strips were used only in a stream of pre-purified nitrogen, to suppress formation and volatilisation of iridium oxide at elevated temperatures [9]. These samples were observed through an optical pyrometer and a filtered binocular microscope during heating, and once quenched were often examined by X-ray diffraction methods as well.

Mild hydrothermal conditions (600 to 1150° C, 5000 to 50 000 psi) were imposed in the low temperature region of the systems studied. The sample to be subjected to hydrothermal treatment was sealed in a 2.5 mm diameter gold tube or 2 mm platinum tube to which was added 15 wt. % H_2O. The walls of these capsules were thin enough to collapse and equalise pressure both inside and outside the capsule. The desired pressure was then applied by pumping water (in a test tube or cold seal bomb) [10, 11] or argon (internally heated device) [12] around the capsules. The water was removed by pressure (leak) quenching, before the temperature quench, in order to build up pressure in the capsules so that all the water present was blown out. This prevented persistence of any intermediate hydrated compounds or hydroxides during cooling. The samples treated by hydrothermal techniques were mixtures pre-reacted at temperatures above or below the run temperature and original mixtures.

It is to be noted that the boundaries determined were not confirmed by measurements at

high temperatures. Thus, high temperature equilibrium situations for all constituents in all possible high temperature arrangements may not have been reproduced in the quenched specimens studied, in spite of the very rapid quenching rates employed. The experimental sluggishness of the decomposition and exsolution reactions in these systems shows that ionic mobilities were sufficiently frozen in during quenching to preserve temperature-composition influences on high-temperature structural relations. This is not to deny that the equilibria preserved may be selective; for example, the quenched specimens in question may be representative of attainment and preservation of structural symmetry equilibria at high temperature, yet may contain very different kinds of point defect structures before and after quenching.

2.3. Product Identification and Characterisation

Portions of heated, quenched samples were examined by X-ray diffraction and optical microscopy techniques, although the great majority of samples investigated were too opaque or fine-grained for the petrographic microscope to be used in a quantitative manner. Therefore, phase identification and characterisation was chiefly dependent upon procedures involving a Norelco diffractometer equipped either with a Geiger or a proportional detector using Ni-filtered Cu Kα radiation and 4° slits.

In certain cases where an exact definition of precision lattice constants was not possible (e.g. for the determination of the solubility-limit of the dioxide in A- or B-type oxides) the proportions of phases present were estimated from patterns run on mechanically mixed synthetic powders compared with those of fired samples. The limit of detectability of dioxide was found to be about 5% in mechanical mixtures and probably 3 mole % for fired (crystalline solution) samples.

Well-crystallised, equilibrated powders within their stability fields were used for determinations of point defect character. Thus, it was necessary to determine lattice parameters (and hence, "X-ray density") and the "bulk density" independently. The peak positions of the high-angle region X-ray profiles determined were indexed and used to calculate a_0 values extrapolated to 180° in 2θ [13]. The parameters thus obtained from the X-ray data were used to calculate the densities of each cubic composition studied, consecutively assuming the appropriate pure interstitial and vacancy models.

Density values calculated above were compared with those pycnometrically measured on equilibrated $\frac{1}{2}$ to 1 g partially sintered samples. Standard calibrated pycnometers of usual design, ranging in volume from 2 to 10 ml were employed in the pycnometric determinations. A dense liquid (usually bromoform) was partially displaced by the sample. It was found essential to de-gas the entire assembly by evacuation before weighing, in order to expel as much of the adsorbed and dissolved gases as possible. The accuracy of the method was checked against the density of single crystal fragments of alumina and quartz. In all cases duplicate density determinations were run on each fired sample as a check on the precision of the method.

Sintered pellets or pellet fragments were used in as many cases as possible. However, such samples were often not available for runs below 1500° C. Because of the very high surface area-to-volume ratios encountered with microcrystalline powders, another technique was devised. Equal amounts by weight of powdered samples were weighed out and pelleted at 7500 psi. These were then cold-pressed at 5 to 20 kbars in a Bridgman anvil apparatus for 5 to 15 min. The runs were then pressure-quenched and removed from the nickel rings used to retain the pellets. Such procedures have resulted in densification of ThO_2-based powdered materials to bulk density values higher than 9.95 g/cm^3 without other appreciable changes occurring. Only wafers which were translucent and bubble-free were used in density determinations by hydrostatic weighing in air and in bromoform, with a sensitive Cahn microbalance.

3. Experimental Results

3.1. Phase Equilibria

A reasonable interpretation of the data* in the system La_2O_3–ThO_2 is represented in fig. 1 [14]. Two intermediate crystalline compounds, $4La_2O_3{:}1ThO_2$(4:1) and $2La_2O_3{:}1ThO_2$(2:1) were found to exist under equilibrium conditions in this system. Both exhibited stability minima. The characteristic powder patterns of these compounds are listed in table I.

The X-ray patterns of quenched melts of the

*Tables listing individual runs have been omitted for brevity. They are available to interested readers on microfilm [14].

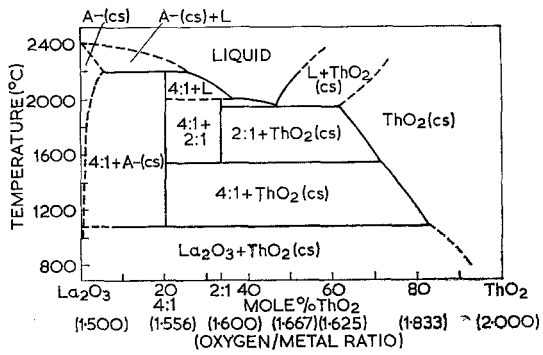

Figure 1 The system La_2O_3–ThO_2.

4:1 compound contained either the patterns of the A-type rare earth oxide structure and the 4:1 compound (rapid quenching procedure) or those of the 4:1 and 2:1 compounds (slow quench). The quenched melt X-ray patterns of the 2:1 compound contained either the patterns of the 4:1 and 2:1 compounds (fast quench) or those of 4:1, 2:1 and ThO_2 crystalline solutions (ThO_2(cs)) (slow quenching procedure). These indications of incongruent melting are represented in fig. 1. The 2:1 compound appears to be stable to a maximum temperature of 2000 $\pm$ 50° C and decomposes at 1525 $\pm$ 25° C. The 4:1 compounds decomposed below about 1150° C and at 2200 to 2250° C.

Attempts were made to define the real composition widths of the single-phase 4:1 and 2:1 compounds by examining compositions near these ratios. No such widths were detectable by the experimental methods employed. Thus, they are represented in fig. 1 as vertical lines (i.e. single-phase stability fields of extremely narrow extent).

The large stability field of the crystalline solution of La_2O_3 in ThO_2 extends to between 35 and 39 mole % in the temperature region 1800 to 1940 $\pm$ 10° C (the eutectic temperature). At the other end of the diagram however, examination of samples fired at 1700 $\pm$ 5° C and then quenched, revealed no measurable crystalline solution in the A-type structure.

The 4:1 and 2:1 compounds have not been reported previously. Moreover, the subsolidus decompositions of the 4:1 and 2:1 compounds are interesting features of the La_2O_3-ThO_2 system. This rare phenomenon in oxide systems has only recently been observed to occur extensively in several rare earth systems, as for example the system Yb_2O_3-CaO [15].

TABLE I Powder diffraction patterns for $4La_2O_3$:ThO_2 and $2La_2O_3$:$1ThO_2$ compounds.

$4La_2O_3$:$1ThO_2$		$2La_2O_3$:$1ThO_2$	
*d*Å	Relative intensity	*d*Å	Relative intensity
3.3634	100	3.3885	15
3.2963	100	3.3022	87
3.0030	65	3.0945	100
2.9497	85	3.0531	100
2.8622	50	2.9308	36
2.8506	50	2.1414	12
2.2210	100	1.9852	12
2.1885	90	1.8497	10
1.8417	60	1.8122	15
1.8069	65	1.7307	20
1.6417	37	1.6945	29
		1.5908	12

Plots of precision lattice parameters versus composition at each isotherm were used to define the position of various phase boundaries in this system. Precision in the high ThO_2 end of the diagram is estimated to be of the order of $\pm$ 0.001 Å, and $\pm$ 0.003 Å for weaker or more indistinct peaks.

The phase diagram shown is in marked contrast to the 1400° C isotherm reported in the literature [1]. The previous investigators did not report the existence of any intermediate compounds in the system. Their firing procedure (from low to high temperature with the highest temperature reached being approximately 1420° C, where only the 4:1 phase is stable) favoured metastable persistence of starting material structures. Compound formation was evidenced in this study only when firing temperatures were well above the lower limit decomposition temperatures of the respective compounds. The assumption of the attainment of equilibrium by "lengthy heating" [1] alone appears to be invalid in this system. The temperatures at which ionic mobilities in these very high melting oxides are expected to become high enough for the solids to become reactive (the Tammann temperature [16]) are approximately 1200° C for La_2O_3, and for ThO_2, 1720° C. Eyring and Holmberg [17] have emphasised that at low temperatures cationic mobility in these materials is too low to be practically useful for reactions involving cationic transport. Thus, interactions requiring metal ion movement would be expected to be slow. A

further factor is that the La_2O_3 used as a starting material in this investigation was of higher purity than in the earlier work referred to (roughly 99.99 + compared to 99% La_2O_3). The chief impurity in the previous study was Ce. The mixing and segregation processes necessary for compound formation and subsequent phase segregation might conceivably have been interfered with by the oxidation-reduction equilibria and transfer processes in Ce_2O_3–CeO_2 [18], in addition to the relatively low temperatures employed. The occurrence of slow reactions, metastability, and hysteresis effects are generally expected in these systems.

Another discrepancy between this and previous work is that the La_2O_3–ThO_2 fluorite-phase crystalline solution field has been reported to extend to approximately 32 mole % La_2O_3 at 1400° C, while the present investigation shows it up to 23 mole %. One possible explanation of this difference is that the quench procedure used on these samples in the present investigation was not very effective. However, it seems unlikely that the quench procedure of previous workers was considerably different. If the lattice parameter data from both investigations is replotted allowing for the stated maximum uncertainties in the lattice parameters, then the solubility limit in both investigations can be set at approximately 30 mole % La_2O_3.

The limiting boundary of the A–La_2O_3 crystalline solution field is not well defined. It was found that the measured lattice parameters for this phase varied from preparation to preparation and were unreproducible. This is unavoidable in phases as hygroscopic as A–La_2O_3.

The results of runs made in the system Gd_2O_3–ThO_2 are summarised as a best interpretation of the data in fig. 2. The most striking feature of the Gd_2O_3–ThO_2 phase diagram is the extensive crystalline solution field of Gd_2O_3 in ThO_2 (i.e. the fluorite field). This field extends from approximately 19 mole % Gd_2O_3 in ThO_2 at 800° C to about 45 mole % Gd_2O_3 in ThO_2 at the eutectic temperature (approximately 2000 ± 50° C) as determined on the strip furnace. The use of the hydrothermal techniques described shows substantial exsolution of the ThO_2-phase as evidenced by the narrower extent of the fluorite-phase at 800° C.

A surprising feature in this system, and one which has never before been noted, is the extensive solid solution field (greater than 30 mole % at 2000° C) in the C-type structure. The saturated C-type rare earth structure contains approximately 38 mole % ThO_2 at the eutectic temperature, 2000° C. It is also interesting to note that the temperature of the polymorphic C-type Gd_2O_3 (cubic) to B-type inversion is raised substantially by increasing the ThO_2 content.

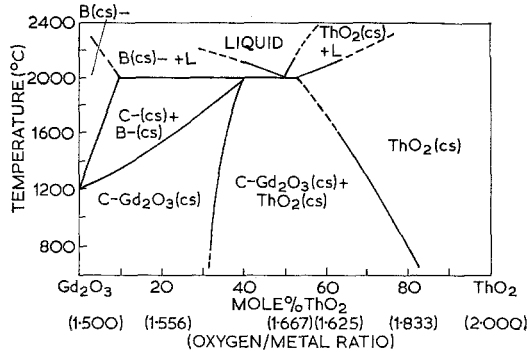

Figure 2 The system Gd_2O_3–ThO_2.

Precision lattice parameter determinations of the fluorite- and C-type structures as a function of temperature and composition were used to locate various phase boundaries in the system. Precision for sharp lines in the ThO_2 crystalline solution region of the diagram is approximately ± 0.001 Å. For weaker and more indistinct lines the uncertainty is ± 0.005 Å maximum.

The results of phase equilibrium investigations in this system may be compared to those previously presented [1]. At 1400° C (the only temperature cited) the extent of crystalline solution of Gd_2O_3 in ThO_2 is given as 33 mole % Gd_2O_3. This agrees favourably with the 30 mole % Gd_2O_3 position of this boundary in the present investigation. The extent of the C-field is much larger than previously reported (25 as against 13 mole % at 1400° C). However, the occurrence of the two-phase, C- + B-crystalline solutions field and one-phase B-crystalline solutions field has not been previously reported in this system. These results might be expected on the basis of previous work [19] in the system Eu_2O_3-ThO_2. The same sequence of phases is reported for this system as in the present study. This is reasonable, since Gd and Eu are neighbours in the lanthanide series, exhibit the same 3+ valence state, have similar ionic radii ($r\ Gd_{3+} = 0.97$ Å, $r\ Eu_{3+} = 0.98$ Å), exist in the

same polymorphic sesquioxide structures (C- and B-types) and have inversion temperatures relatively close to one another. At 1400° C the extent of Eu_2O_3 solubility in ThO_2 crystalline solution is 32 mole %, as compared to the 30 mole % Gd_2O_3 boundary position. The 1400° C boundary between C–Eu_2O_3 (cs) and C–Eu_2O_3 (cs) + ThO_2 (cs) is reported as 77 mole % Eu_2O_3. The corresponding boundary in the Gd_2O_3–ThO_2 system is at 66 mole % Gd_2O_3. The boundaries of the C-phase are shown for the Eu_2O_3–ThO_2 system at 85 and 98 mole % Eu_2O_3 at 1400° C. The equivalent boundaries in the Gd_2O_3–ThO_2 system are shown in the present investigation at 88 and 98 mole % of Gd_2O_3. Thus, these rather analogous systems agree very closely with one another.

The greatest cause of the discrepancy with earlier work is most probably in the manner and extent of approach to equilibrium. Previous investigators [1] claimed probable attainment of equilibrium on the one hand and yet reported it to be impossible to define the lattice parameter of the various compositions in the Gd_2O_3–ThO_2 system on the other, which allowed them (at best) to approximate the positions of phase boundaries. High-pressure, high-temperature water (under "hydrothermal conditions") was used as a catalyst in all systems included in the present study to aid in resolving subsolidus phase equilibria in the low-temperature (sub-Tammann temperatures) region of these diagrams.

The comparison of phase relationships reported for this system might be further clouded by the lower purity of Gd_2O_3 previously used (approximately 99% Gd_2O_3, Sm as chief impurity) compared with that used in the present study (0.1% maximum impurities, as other rare earths).

Noteworthy features in the system Yb_2O_3–ThO_2 are moderate solubility of Yb_2O_3 in ThO_2 (approximately 10 mole % Yb_2O_3 at 1800° C), and small solubility of ThO_2 in Yb_2O_3 (approximately 3 mole % ThO_2 at 1800° C). No compound formation or extensive crystalline solution fields exist in this system. The strip furnace was used in the estimation of the liquidus curves and the position of the eutectic. The liquids in this system are not quenchable, thus this method, with its dependence upon visual observation of rounding and collapsing of particle aggregates (on the heated strip through a filtered binocular microscope) to get indications of liquidus temperature, is only an approximate one. In the determination of the solidus, compositions near the eutectic were used in order to take advantage of the large amounts of liquids formed which were clearly seen.

The experimentally determined diagram is presented in fig. 3.

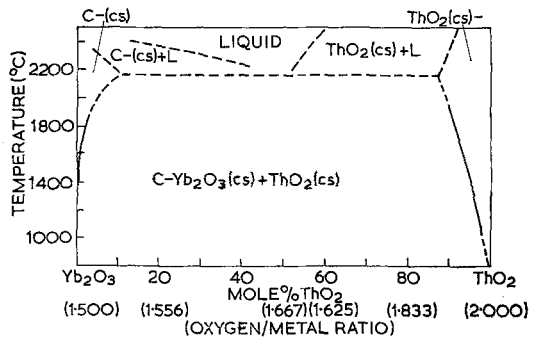

Figure 3 The system Yb_2O_3–ThO_2.

Definition of the boundary between the two stability fields (C–Yb_2O_3 (cs) and ThO_2 (cs) and the fluorite stability field) was accomplished by plotting precision lattice parameters versus composition, over a wide range of temperatures. The boundary between the C–Yb_2O_3 (cs) field and the two-phase field specified above was similarly determined.

Previous work on the Yb_2O_3–ThO_2 system was conducted near 1400° C. Yb_2O_3 was found to be soluble in ThO_2 to the extent of approximately 5 mole %, and ThO_2 in C–Yb_2O_3 to a very small degree (approximately 2 mole %). These limits agree (within experimental error) with those reported in this investigation. It must be pointed out that the appearance of the plots of a_0 versus composition for this system can be deceptive when the solubility limits are very small. Evaluation of data reported with extremes of the limits of accuracy applied could change the boundary positions drastically. However, the data as presented and determined follows the trends represented by the lines included in the diagrams reported here. Attainment of equilibrium in previous work is in doubt for several reasons. The fired preparations described in the literature were not homogeneous to start with. It was thought that traces of C-phase worked as nuclei to hasten dissolution within the quenching time used [19]. Thus, more C-phase comes out in the quenched phase than really exists at the

higher temperature. Secondly, quenching times reported were relatively long. Indeed, the fastest quench claimed was from 1400 to 500° C in 20 sec (i.e. 45°/sec) which strengthens the promoting effect of the C-phase nuclei. Finally, the earlier experiments showed different results in approaching the "equilibrating" temperature from above and below. This is not surprising since the temperature desired is very near that at which the Yb^{3+} cations are just mobile, as gauged by the Tammann temperature (1300° C for Yb_2O_3, 1720° C for ThO_2).

3.2. Point Defect Descriptions for Fluorite-Structure Crystalline Solutions

The change in value of the lattice constant of a cubic material depends to a first approximation linearly upon the concentrations of point defects of major importance in the material [20, 21]. Thus, precision lattice parameters determined for the systems of interest were used in an analysis of the predominant point defect situations present in the various fluorite (cubic) microcrystalline solution phases existing at equilibrium in them. One important assumption made was that the defect chemistry is defined by the concentration of the impurity (i.e. second-phase) dissolved in the host phase. This implies that the oxide end members do not themselves exhibit significant deviations from stoichiometry. The cation concentration ratios as determined in various fired samples were in good agreement with those of the starting mixtures. However, the question of the deviation from ideally expected stoichiometry of the anion (oxide) sublattice was not studied experimentally. It is felt that any deviation from stoichiometry for these particular oxides (ThO_2, La_2O_3, Gd_2O_3, Yb_2O_3) is quite insignificant in the definition of the defect situations present in these materials. The measurable but thermodynamically insignificant non-stoichiometric $ThO_{1.998}$ exists only above 2500° C, and evaporates quite stoichiometrically below this [22]. La_2O_3 taken as an example of a rare earth sesquioxide also evaporates stoichiometrically at the temperatures of this investigation [23].

The process of crystalline solution formation between the rare-earth sesquioxides and thoria resulting in a fluorite-structure phase may be thought of as occurring by one of two schemes. To preserve charge balance, either anion vacancies or cation interstitials must form. These rationalisations may be represented schematically either as crystalline solutions with complete cation lattices and anion vacancies, or as crystalline solutions with complete anion lattices and complete cation lattice arrangements, and excess cations in interstitial positions. It has been concluded that this preservation of the stoichiometry is the case in Ln_2O_3–ThO_2 crystalline solutions [24, 25]. Qualitative comparisons of X-ray diffraction intensities revealed no special segregation or orientation effects of impurity (i.e. second-phase) cations to the host oxide cation.

Once the specific extreme defect models (vacancies or interstitials) were hypothesised for the fluorite-type crystalline solutions under investigation, the densities of these materials were calculated using the experimentally determined precision lattice parameters for computation of the unit cell volume, and the chemical composition for computation of the unit cell formula weight. One of these "X-ray densities" was calculated; they were compared with those experimentally determined. These results are summarised in figs. 4, 5, and 6 for selected isotherms of the systems studied.

In the range of densities encountered (approximately 7 to 10 g/cm³) precision was of

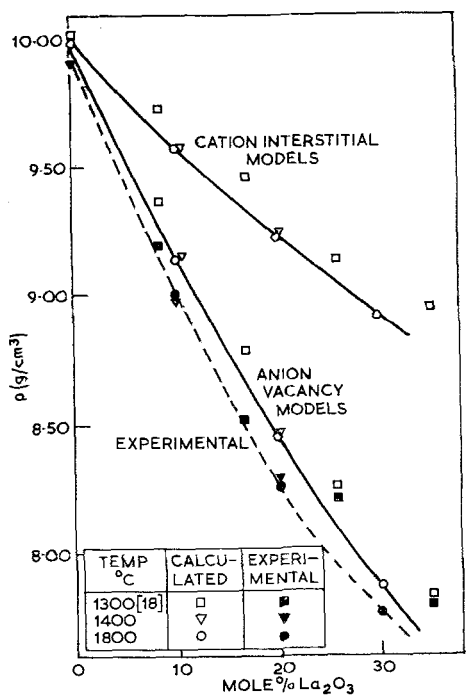

Figure 4 Density-composition curves for crystalline solutions of La_2O_3 in ThO_2.

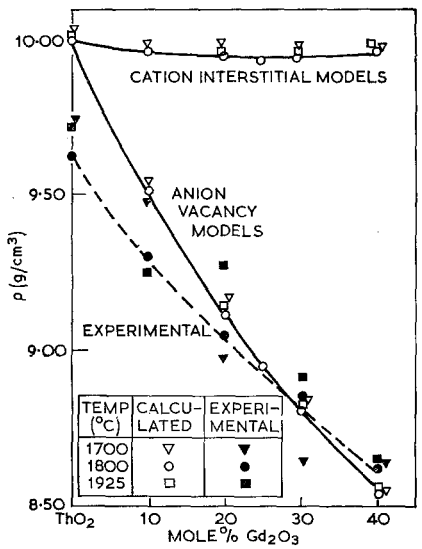

Figure 5 Density-composition curves for crystalline solutions of Gd_2O_3 in ThO_2.

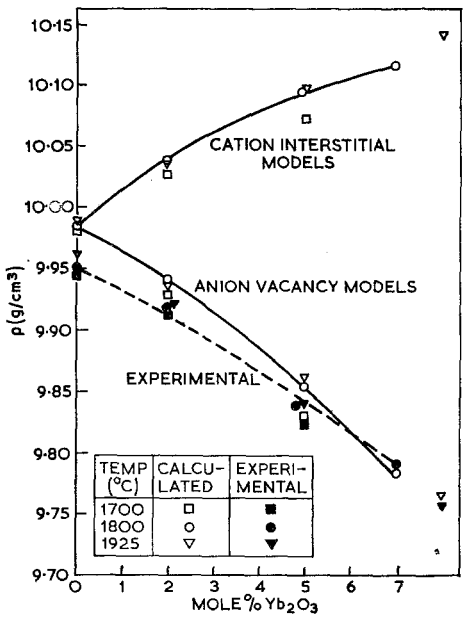

Figure 6 Density-composition curves for crystalline solutions of Yb_2O_3 in ThO_2.

the order of $\pm$ 0.05 g/cm³. This level of precision is attainable with the method outlined above, and has been reported by other workers on similar samples using a displaced-liquids method [26] (as in the present study) or by displacement of a known volume of helium [27]. The density dependence on composition of samples quenched from the temperature cited is such that there is good agreement between the pure* anion vacancy models (calculated from X-ray data) and the experimentally determined density values. This agreement is of the order of 1.5% in the system La_2O_3–ThO_2, with the pycnometrically determined values always lower than those calculated for the anion vacancy model. This lower value is expected from the evaluation of the various systematic errors that are normally introduced in such measurements (e.g. porosity, air films adsorbed on surfaces, etc). The effect of presence of voids does not prohibit use of the pycnometric technique described above to determine the change in density (and hence the defect nature) as a function of composition and firing temperature, since the void volumes have been found to be rather constant during such isothermal compositional variations in very similar oxide crystalline solutions having fluorite structures [28]. It was also found that the densities of pellet fragments of pressed powder in these systems generally were nearly equal to those determined for well de-gassed powders. Similar agreement exists between these results and those reported by Hund and Dürrwächter [29] for the La_2O_3–ThO_2 system across the 1300° C isotherm. In general, the pycnometrically-determined curves for the fluorite crystalline solutions field fell on or below those of the calculated anion vacancy model (within experimental error) in all three systems and in Hund's study [29]. The few experimental points not obeying this trend might be the result of such considerations as appearance of random errors, sintering peculiarities, or more importantly, contributions of more than one "pure" defect situation to the overall picture. These results are descriptions based upon end-member or extreme models of defect situations. The approach of the fluorite to C-type structure transition may thus be rationalised on a reasonable structural basis (i.e. subtraction of anions from the oxide lattice).

4. Discussion and Conclusions

A summary of crystalline solubility limits for Ln_2O_3 in ThO_2 (fluorite field) is presented in

*The term "pure" is used advisedly, suggesting here that one type of defect appears to predominate to such an extent that other defect situations are not suggested and cannot be differentiated by the methods used. In principle, of course, finite concentration of all types are present, including a distribution of cluster sizes of each type.

fig. 7 as a function of (Goldschmidt) ionic radius. Although almost all the previous work reported [1, 19, 24, 30-33] has been done at only one temperature, or at best in a very narrow temperature range (in the vicinity of 1200 to 1400° C), theories have been developed as to conditions for, and extent of crystalline solution formation in fluorite-structure dioxide systems on the basis of cell parameter and ionic radii alone. For example, it has been reported that continuous crystalline solutions will exist in such systems if the difference in lattice parameter of the end-member components does not exceed $\pm 2\frac{1}{4}\%$ [1]. It is interesting to note that these investigators point out that the systems La_2O_3–ThO_2, Ce_2O_3–ThO_2, Pr_2O_3–ThO_2 and Nd_2O_3–ThO_2, while falling within the $\pm 2\frac{1}{4}\%$ rule do not obey it. These failures are usually dismissed as a consequence of rare earth oxide polymorphism. In fact, these generalisations are of very limited validity since they imply that the temperature dependence of the equilibrium relations is negligible. This is, of course, completely erroneous, as can be seen from figs. 1, 2 and 3. Such theories seem to be extensions of Goldschmidt's miscibility rules. (The end-member compounds must exhibit the same structure as one another and their cationic radii must be within 15% of one another [34].) They were gradually modified to the idea that crystalline solution formation depends on the matching of unit cell dimensions or multiples of such dimensions. However, as more and more systems werre studied, this historical need for similarity in formula, structural types, and size have been eliminated as prime conditions for crystalline solution formation. It is unfortunate that the "unit cell matching" oversimplification developed as strongly as it did.

Dietzel [35] used the concept of field strength (FS) as an aid in explaining and predicting trends in compound formation, relative extent of crystalline solubility, melting stability, and melting points. Ionic field strength is defined by $FS = Z/A^2$, where Z is the valence of a cation and A is the sum of the cationic and anionic radii. The difference in relative field strength (i.e. FS cation 1 — FS cation 2 = ΔFS) is an indication of the number of compounds formed in a binary system. Compound formation is generally expected above $\Delta FS = 0.3$, with an

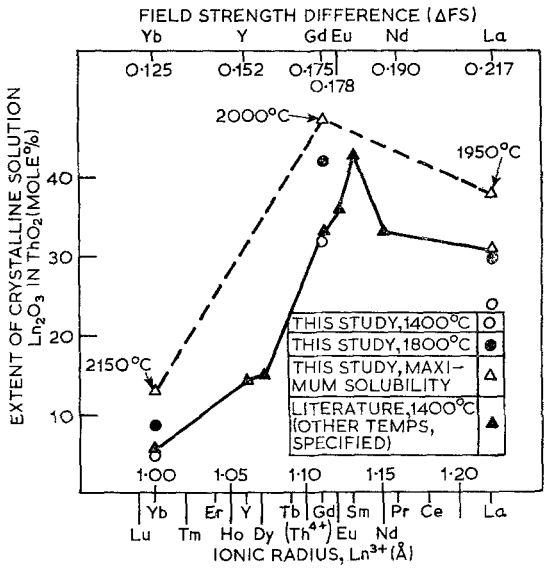

Figure 7 Extent of fluorite crystalline solution in Ln_2O_3–ThO_2 systems.

increase in the number formed as ΔFS increase [36]. The FS's of the tervalent rare earth ions and Th^{4+}, and the relative ΔFS's of the rare earth ions (Th^{4+} as basis of comparison) have been calculated and are shown in table II.

Although none of these ΔFS values did reach the 0.3 level, the La^{3+}–Th^{4+} set had the highest value, 0.23. On this basis, out of any of the rare earth sesquioxide – ThO_2 systems the La_2O_3 case would be most expected to show compound formation*. The important phase diagram feature of major interest in this study is the extent of crystalline solubility. Dietzel concluded that ΔFS values of approximately ± 0.05 usually indicated extensive or complete crystalline solution. It can be seen from a correlation between these values in table II and results previously summarised, that the opposite is true in Ln_2O_3–ThO_2 systems. Sc_2O_3 is only slightly soluble in ThO_2 ($\Delta FS = 0.069$); considerably greater extents of crystalline solution fields of Ln_2O_3 in ThO_2 at a particular temperature are shown for Gd^{3+} ($\Delta FS = 0.19$) and La^{3+} ($\Delta FS = 0.23$) than for Yb^{3+} ($\Delta FS = 0.18$). A similar conflict with the solubility rule was found by Barry in the systems La_2O_3–CaO, Gd_2O_3–CaO, and Yb_2O_3–CaO [15]. Thus, this rule does not seem to hold for such binary

*Several authors found sequences of the general formula M_nO_{2n-2} in Ce, Pr and Tb oxide systems [43, 44]. The 2:1 phase is M_5O_8; the 4:1 phase is not in this series. These compounds probably result from point defect ordering in the closely related A-type and fluorite-type crystalline solution structures [45].

TABLE II Relative field strengths of tervalent rare earth ions.

Cation	r cation Å [13]	FS (anion = 0^{2-})	ΔFS
Sc^{3+}	0.83	0.649	0.033
Y^{3+}	1.06	0.530	0.152
La^{3+}	1.22	0.465	0.217
Ce^{3+}	1.18	0.480	0.202
Pr^{3+}	1.16	0.487	0.195
Nd^{3+}	1.15	0.492	0.190
Pm^{3+}	1.14	0.496	0.186
Sm^{3+}	1.13	0.500	0.182
Eu^{3+}	1.12	0.504	0.178
Gd^{3+}	1.11	0.507	0.175
Tb^{3+}	1.09	0.516	0.166
Dy^{3+}	1.07	0.526	0.156
Ho^{3+}	1.05	0.534	0.148
Er^{3+}	1.04	0.538	0.144
Tm^{3+}	1.02	0.548	0.134
Yb^{3+}	1.00	0.557	0.125
Lu^{3+}	0.99	0.561	0.121
(Th^{4+})	(1.10)	(0.682)	—

0^{2-} radius taken as 1.32 Å

systems, where valences are not matched and major defects are created by the substitution.

The failure of the simple field strength approach is a further indication of the complexity in predicting and explaining phase equilibria and crystal chemical relations in these systems. Any comprehensive theories or rules regarding them must be tested with respect to number of compounds existing in a system and their stoichiometries, solid-state transition behaviour, decomposition and melting relationships as well as solubilities of adjacent compounds [36]. The influence of polarisation may be specified in a characterisation of ions in crystal chemical studies, along with ionic sizes and ionic field strengths. The percentage polarisation [37] is an indication of electron shell distortion, the reference state of which is polarisation = 100 for the ideal ionic bond. On this basis, it is expected that all of the rare earths would be expected to behave alike. (Percentage polarisation varies from 83 to 87 for the rare earth tervalent ions.) Large crystalline solution stability fields, indicative of similar chemical and structural properties exist in the La_2O_3–, Gd_2O_3–, and Yb_2O_3–ThO_2 binaries, even though a difference exists between the electronegativities of the 3^+ and Th^{4+} ions. This is in contrast to the very narrow crystalline solution field found in the Sc_2O_3–ThO_2 system [30] in spite of the identity of electronegativity values for Sc^{3+} and Th^{4+}. Thus, the Pauling electronegativity parameter does not add to the understanding or prediction of phase equilibria in the systems studied. A substitution of "crystallochemical electronegativities" (based upon lattice energies) calculated using Kapustinskii's formulae [38] and the lattice energies listed by Ladd and Lee [39] shows little difference in values for the rare earth ions (20.3 kcal/mole for La^{3+}, 20.8 for Gd^{3+}, 21.1 for Yb^{3+}) and is also of no aid in these systems.

TABLE III Lattice energies of oxides (after Ladd and Lee [39]).

Oxide	r_0 Å (mean anion-cation distance)	Lattice energy kcal/mole	(Lattice energy R_2O_3- lattice energy ThO_2) ÷(lattice energy ThO_2)
La_2O_3	2.62	3011	0.212
Gd_2O_3	2.322	3138	0.262
Yb_2O_3	2.241	3251	0.308
ThO_2	5.597	2485	—

The values of r_0 are weighted mean values used to overcome the lack of unique distance in the A-type structure.

Haven [40] has made a semiquantitative treatment of the crystalline solution problem for Mg-Li halides. It was found that the extent of solubility runs parallel to the loss in co-ordination energy when solute is dissolved in solvent for these systems. The desired final state is one in which the energy of solution is at a minimum. Haven considered this energy of solution to be the sum of the differences of Madelung energy, repulsive energy and polarisation energy terms for the solute and solvent structures. If lattice energies could be used as a rough guide in this kind of an argument (since Madelung, polarisation, and repulsion terms come into play in both) then it can be seen from table III that Yb_2O_3 could be expected to be less soluble than either La_2O_3 or Gd_2O_3 in ThO_2. Since the Madelung constant for the A-type structure is 26.4 in comparison to 24.3 for the C-type [39], the Madelung energy difference contribution should be least for La_2O_3–ThO_2 (a solubility-favouring factor). The repulsion energy (roughly proportional to $1/r^k$ should be highest for the Yb_2O_3 case on the basis of interionic distances. However, the co-ordination number has been changed from seven to eight upon solution of La^{3+} in ThO_2, changing the repulsive energy in the dissolved state to roughly 8/7 times that of the

repulsive energy in the solute (A-type) structure, while the co-ordination number change for Gd^{3+} and Yb^{3+} is from six to eight upon solution of either of these ions in ThO_2. Thus, the repulsive energy in the crystalline solution for these two solutions is approximately 8/6 greater than the repulsive energy in the solute (C-type) structures. For the three systems studied, the repulsive energy terms should therefore be very near one another. The comparatively large contribution of the Madelung energy term differences thus must be overcome by the remaining polarisation energy term to markedly different degrees for crystalline solution stability. The solvent lattice is thought of as being polarised by the lattice defects formed in the dissolving of the solute ions of different charge.

The specific crystal structure exhibited by a substance corresponds generally to the state of lowest lattice energy. However, when ionic surroundings change drastically, energy is needed to dissolve solute ions into the solvent structure in order to force these solute ions to adapt to their new surroundings. Thus, the common observation of extensive, and often complete miscibility between isotypic solids is to be expected. The fact that "anomalous" crystalline solutions do exist points out that the energy loss in bringing ions from the solute to solvent configuration must be compensated for by other energy terms (repulsive and polarisation terms). The polarisation energy effect is comparable to that of hydration in electrolytic solutions as the main factor is dissolving ionic compounds. This polarisation energy term is approximately inversely proportional to the anion-cation distance [40] (among other factors constant for the three systems in question). Thus, the biggest difference in polarisation (of opposite sign to the lattice energy terms) would be for the Yb_2O_3–ThO_2 system (minimum solubility).

Although parallels may be drawn between Haven's work and this study, at the present an exact computation of such terms for much less complicated systems (e.g. highly dilute alkali halides + alkaline earth halides) has proven to be very difficult [41].

The crystalline solution fields existing over large ranges of temperature and composition in these systems are reasonable from another viewpoint. Bertaut has remarked that vacancy formation and ordering can liberate amounts of energy so large that the entropy contribution to the free energy would be comparatively negligible [42]. Thus, some degree of stability is afforded to these defect crystalline solutions by defect formation at high temperatures. That these effects are not noticeable at low temperatures is due to the fact that true equilibrium cannot always be attained in real systems because of the interplay between kinetic and equilibrium considerations. These point defects can be ordered and formed only at temperatures at which sufficient diffusional mobility exists. The formation of point defects by inclusion of impurity (i.e. major second-phase) ions helps stabilise these extensive crystalline solutions, and may act as blocking points for electronic transfers between minor alternative ion impurities. Thus, even metastability and randomness could probably persist in these systems upon quenching. The development of hypotheses concerning various types of point defects as a means of compensating for the different stoichiometries and charges of the end-member oxide cations is extremely important in interpreting the solid state chemistry of these systems. However, such schemes are really rationalisations dependent upon experimentally determined equilibria.

It is clear from this investigation that a need exists for critical review and evaluation of concepts currently held concerning formation and extent of crystalline solutions in ionic oxide systems, as well as general criteria for predictions of phase equilibria in these materials.

References

1. G. BRAUER and H. GRADINGER, *Z. anorg. Chem.* **276** (1954) 209.
2. K. KIUKKOLA and C. WAGNER, *J. Electrochem. Soc.* **104** (1957) 309.
3. H. MÖBIUS, *Z. Chem.* **4** (1964) 81.
4. W. D. KINGERY, J. PAPPIS, M. E. DOTY, and D. C. HILL, *J. Amer. Ceram. Soc.* **42** (1959) 393.
5. A. F. WELLS, "Structural Inorganic Chemistry" (Oxford University Press, 1962).
6. W. LUTH and C. INGAMELLS, *Amer. Min.* **50** (1965) 255.
7. M. L. KEITH and R. ROY, *ibid* **39** (1954) 1.
8. H. ROBERTS and G. MORERY, *Rev. Sci. Instr.* **1** (1930) 576.
9. J. CHASTON, *Platinum Met. Rev.* **9** (1965) 51.
10. O. TUTTLE, *Bull. Geol. Soc. Amer.* **60** (1949) 1727.
11. R. ROY, D. ROY, and E. OSBORN, *J. Amer. Ceram. Soc.* **33** (1950) 152.
12. J. GOLDSMITH and H. HEARD, *J. Geol.* **69** (1961) 45.
13. A. TAYLOR and H. SINCLAIR, *Proc. Phys. Soc.* **57** (1945) 126.
14. A. M. DINESS, Ph.D. thesis, The Pennsylvania State University (1967).

15. T. BARRY, Ph.D. thesis, The Pennsylvania State University (1964).
16. G. TAMMANN, *Z. anorg. Chem.* **157** (1926) 321.
17. L. EYRING and B. HOLMBERG, in "Nonstoichiometric Compounds", edited by R. Ward (American Chemical Society, Washington, 1963) p. 46.
18. G. BRAUER and K. GINGERICH, *J. Inorg. Nuclear Chem.* **16** (1960) 87.
19. K. GINGERICH and G. BRAUER, *Z. anorg. Chem.* **324** (1963) 48.
20. P. H. MILLER JR and B. R. RUSSELL, *J. Appl. Phys.* **23** (1952) 1163.
21. J. D. ESHELPY, *ibid* **24** (1953) 1249.
22. R. J. ACKERMANN, E. G. RAUH, R. J. THORN, and M. C. CANNON, *J. Phys. Chem.* **67** (1963) 762.
23. H. W. GOLDSTEIN, P. N. WALSH, and D. WHITE, *ibid* **65** (1961) 1400.
24. J. LÈFEVRE, Ph.D. thesis, University of Paris (1963).
25. U. CROATTO and M. BRUNO, *Ricerca Sci.* **18** (1949) 578. Abstract in *C.A.* **43** 8789a.
26. W. BILTZ, *Z. anorg. Chem.* **121** (1922) 259; W. BILTZ and E. BUCK, *ibid* **134** (1924) 130.
27. I. FERGUSON and P. FOGGS, *J. Chem. Soc.* (1957) 3679.
28. L. LYNDS, W. A. YOUNG, J. S. MOHL, and G. G. LIBOWITZ, in "Nonstoichiometric Compounds", edited by R. WARD (American Chemical Society, Washington, 1963) p. 58.
29. F. HUND and W. DÜRRWÄCHTER, *Z. anorg. Chem.* **265** (1951) 67.
30. W. TRZEBIATOWSKI and R. HORYŃ, *Bull. de L'Academiè Polonaise des Sciences* **XIII** (1965) 303.
31. H. MÖBIUS, *Z. Chem.* **5** (1964) 194.
32. F. HUND and R. MEZGER, *Z. phys. Chem.* **201** (1952) 268.
33. W. VAN GOOL, *J. Phys. and Chem. Solids* **27** (1966) 581.
34. V. M. GOLDSCHMIDT, *Skrifter utgit ov det Norske Videnskap-Akademi i Oslo, Matem Naturvid.* Klasse I (1926) 83.
35. A. DIETZEL, *Z. Elektrochem.* **48** (1942) 9.
36. K. S. VORRES, *J. Amer. Ceram. Soc.* **46** (1963) 410.
37. L. PAULING, "The Nature of the Chemical Bond" (Cornell University Press, Ithaca, 1960).
38. A. F. KAPUSTINSKII, *Quart. Rev.* X (1955-6) 283.
39. M. F. C. LADD and W. H. LEE, *J. Inorg. Nuclear Chem.* **23** (1961) 199.
40. Y. HAVEN, *Rec. Trav. chim.* **69** (1950) 1505.
41. P. BRAUER, *Z. Naturforsch.* 7a (1952) 372; *idem, ibid*, 6a (1951) 562.
42. E. F. BERTAUT, *Acta Cryst.* **6** (1953) 557.
43. D. J. M. BEVAN, *J. Inorg. Nuclear Chem.* **1** (1955) 49.
44. L. EYRING *et al*, *J. Amer. Chem. Soc.* **76** (1954) 3890, 5239, 5242; *idem, ibid*, **83** (1961) 2219.
45. J. S. ANDERSON, in "Nonstoichiometric Compounds", edited by R. WARD (American Chemical Society, Washington, 1963) p. 9.